

# CONTEXTUAL LEARNING

Rico Jonschkowski\*, Sebastian Höfer\* & Oliver Brock

Robotics and Biology Laboratory  
Technische Universität Berlin  
Berlin, Germany

{rico.jonschkowski, sebastian.hofer, oliver.brock}@tu-berlin.de

## ABSTRACT

Supervised, semi-supervised, and unsupervised learning estimate a function given input/output samples. Generalization to unseen samples requires making prior assumptions about this function. However, many priors cannot be defined by only taking the function, its input, and its output into account. In this paper, we propose *contextual learning*, which uses *contextual data* to define such priors. Contextual data are neither from the input space nor from the output space of the function, but include useful information for learning it. We can exploit this information by formulating priors about how contextual data relate to the target function. Incorporating these priors regularizes learning and thereby improves generalization. This facilitates many challenging learning tasks, in particular when the acquisition of training data is costly or when effective learning requires prohibitively large amounts of data. The first contribution of this paper is a unified view on contextual learning, which subsumes a variety of related approaches, such as multi-task and multi-view learning. The second contribution is a set of patterns for utilizing contextual learning for novel problems. The third contribution is a systematic experimental evaluation of these patterns in two supervised learning tasks.

## 1 INTRODUCTION

An important branch of machine learning research focuses on supervised learning, estimating functions from sets of input/output samples with the goal of predicting the correct output for new inputs. However, generalization to unseen samples always requires prior assumptions about the target function (Mitchell, 1980). By incorporating stronger priors into machine learning, we can learn from less input/output samples or solve more challenging problems. But discovering useful priors is difficult, especially if we limit our focus to the input and output of the target function.

For many problems, there are additional data  $\mathbf{c}$  available that are neither the input  $\mathbf{x}$  nor the output  $\mathbf{y}$  of function  $f$ . These additional data  $\mathbf{c}$  carry valuable information about how  $f$  maps  $\mathbf{x}$  to  $\mathbf{y}$ , as illustrated in Fig. 1. We refer to this kind of data as *contextual data*. Examples for contextual data are (i) intermediate results computed by the true underlying  $f$ , (ii) output of a related function (with input  $\mathbf{x}$ ) that shares computations with  $f$ , (iii) input of a related function (with output  $\mathbf{y}$ ) that shares computations with  $f$ , or (iv) relations between inputs  $\mathbf{x}_i$  and  $\mathbf{x}_j$  or between outputs  $\mathbf{y}_i$  and  $\mathbf{y}_j$ .

**Example:** Suppose we want to estimate a function from the input/output samples:  $3 \mapsto 14$ ,  $5 \mapsto 30$ , and  $2 \mapsto 9$ . From looking at these data, it is not immediately obvious what the true underlying function is. However, if we provide contextual data and the prior that these data correspond to intermediate values that  $f$  computes, in this case  $3 \mapsto 9 \mapsto 14$ ,  $5 \mapsto 25 \mapsto 30$ , and  $2 \mapsto 4 \mapsto 9$ , we see that the function first squares its input and then adds five to intermediate result,  $f(\mathbf{x}) = \mathbf{x}^2 + 5$ . Contextual data together with a prior about how the data relate to  $f$  reveal the underlying function.

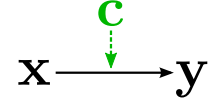


Figure 1: Context  $\mathbf{c}$  is informative about the function from input  $\mathbf{x}$  to output  $\mathbf{y}$

\*The first two authors contributed equally to this work.

Incorporating such priors about how  $\mathbf{c}$  relates to  $f$  is what we call *contextual learning*. By enforcing that the learned function is consistent with these priors, we regularize learning and thereby improve generalization. There are a number of approaches in the literature that, often implicitly, follow the contextual learning paradigm and demonstrate impressive results. This paper connects these lines of work and makes the underlying paradigm explicit.

The first contribution of this paper is a rigorous formalization of the contextual learning paradigm. This formalization includes a set of contextual learning patterns. Some of these patterns can be found in prior work, others represent novel ways of learning with contextual data. These novel patterns therefore represent the second contribution. Our third contribution is a systematical evaluation and comparison of these patterns in supervised learning tasks. We hope that these contributions taken together facilitate further development of the contextual learning idea and enable the transfer of the proposed contextual learning patterns to novel learning problems.

## 2 BACKGROUND

Before providing a detailed explanation of contextual learning, we would like to discuss its relationship to other approaches in machine learning. Since we argue that additional data provide a means of incorporating priors, we begin with a discussion about the role of priors in machine learning.

Machine learning methods are only able to generalize beyond observed data by incorporating priors about the target function  $f$ . Although not always stated explicitly, prior knowledge about  $f$  is reflected in every component of a machine learning approach: in the hypothesis space (e.g. by defining features, kernels, neural network structure), in the generation of training data (e.g. by data augmentation), in the learning procedure (e.g. by learning rate schedule), and in the learning objective (e.g. by including a regularization loss).

In this paper, we focus on incorporating priors into the learning objective by exploiting additional data. This idea per se is not new, and at the very heart of *unsupervised* and *semi-supervised learning*. Those paradigms, however, focus on using additional unlabeled *input* data, whereas contextual learning explicitly considers data that is neither input nor output data of the target function.

There are machine learning approaches that fit our definition of contextual learning, e.g. *multi-task learning*, *multi-view learning*, or *slow feature analysis*. We do not consider contextual learning to be an alternative to these approaches; instead, we provide a unified view that connects these seemingly different approaches, and extract generic patterns from them, which we describe in Section 4.

## 3 CONTEXTUAL LEARNING

In contextual learning we learn a function  $f : \mathbf{x} \rightarrow \mathbf{y}$  by minimizing two objective functions, the *main objective*  $\mathcal{L}_f$  and the *contextual objective*  $\mathcal{L}_c$ :

$$\operatorname{argmin}_{\phi, \psi} \mathcal{L}_f(\phi, \psi \mid \{\mathbf{x}_i, \mathbf{y}_i\}_{i=1}^N), \quad (1)$$

$$\operatorname{argmin}_{\phi, \beta} \mathcal{L}_c(\phi, \beta \mid \{\mathbf{x}_i, \mathbf{y}_i\}_{i=1}^N, \{\mathbf{c}_j\}_{j=1}^M). \quad (2)$$

Note that both objectives share the function  $\phi$ ; this is important because  $\phi$  links the two objectives during learning. We will now explain the objectives and the involved symbols step by step.

To define  $\mathcal{L}_f$ , we assume a supervised learning setting, in which the goal is to estimate a function  $f : \mathbf{x} \rightarrow \mathbf{y}$  from a set of  $N$  input/output pairs  $\{\mathbf{x}_i, \mathbf{y}_i\}_{i=1}^N$ . Then,  $\mathcal{L}_f$  corresponds to a standard supervised learning objective, e.g. mean-squared error for regression, and hinge loss for classification.

The contextual objective is captured by  $\mathcal{L}_c$ , which depends on *contextual data*  $\mathbf{c}$ . These data are neither from the input space nor from the output space of  $f$  but carry valuable information about  $f$ , and are only needed for learning, not for prediction. Hence, the training data include  $M$  context samples in addition to the  $N$  input/output pairs,  $D = (\{\mathbf{x}_i, \mathbf{y}_i\}_{i=1}^N, \{\mathbf{c}_j\}_{j=1}^M)$ . Each of the context sample relates to one or more input/output samples, commonly  $M = N$  or  $M = N^2$ . To exploit  $\mathbf{c}$  for learning  $f$ , we formulate priors about how  $\mathbf{c}$  relates to  $f$  in the contextual objective  $\mathcal{L}_c$ . In order to express the desired relation of  $\mathbf{c}$  and  $f$ , we split  $f$  into two functions,  $\phi$  and  $\psi$ , where  $\phi$  maps  $\mathbf{x}$  to an intermediate representation  $\mathbf{s}$ , and  $\psi$  predicts  $\mathbf{y}$  based on  $\mathbf{s}$ , hence  $\mathbf{y} = f(\mathbf{x}) = \psi(\phi(\mathbf{x})) = \psi(\mathbf{s})$ .

This enables us to relate  $\mathbf{c}$  to function  $\phi$  which is shared by  $\mathcal{L}_f$  and  $\mathcal{L}_c$ . To give more flexibility for relating  $\phi$  and  $\mathbf{c}$  in  $\mathcal{L}_c$ , we introduce the auxiliary function  $\beta$ . The exact form of  $\mathcal{L}_c$  and  $\beta$ , and the relationship of  $\phi, \beta$  and  $\mathbf{c}$  depends on the particular *contextual pattern* that is applied (Section 4).

Note that we intentionally kept this formalization narrow to improve readability. It is straightforward to extend the ideas presented here to a reinforcement learning setting, to multiple types of contextual data, to multiple intermediate representations, and to more than one contextual learning objective.

### 3.1 TRAINING PROCEDURES

Since contextual learning requires us to optimize multiple learning objectives affected by different subsets of training data and functions, we need appropriate training procedures. We have identified three common training procedures that differ with respect to the order in which they (i) optimize the two objectives and (ii) modify the functions  $\phi, \psi$ , and  $\beta$ :

In the **decoupled procedure**, we first optimize the contextual objective  $\mathcal{L}_c(\phi, \beta | \{\mathbf{x}, \mathbf{y}\}, \{\mathbf{c}\})$ , while adapting  $\phi$  and  $\beta$  to learn the intermediate representation  $\mathbf{s}$ . Then, we optimize the main objective  $\mathcal{L}_f(\phi, \psi | \{\mathbf{x}, \mathbf{y}\})$ , while keeping  $\phi$  (and  $\beta$ ) fixed. This simple procedure is only applicable if the contextual objective provides enough guidance to learn a task-relevant representation  $\mathbf{s}$ .

To alleviate this problem, **pre-train and finetune** first applies the decoupled procedure, but then optimizes  $\mathcal{L}_f(\phi, \psi | \{\mathbf{x}, \mathbf{y}\})$  while adapting  $\phi$ , too, in order to fine-tune  $\mathbf{s}$  for the task. This strategy is popular in deep learning as unsupervised pre-training (Erhan et al., 2010) and can be applied analogously for contextual learning. For this procedure to have an effect,  $\mathcal{L}_f$  must not be convex (otherwise, the pre-training step would be unlearned).

Finally, **simultaneous learning** jointly trains  $\phi, \beta$  and  $\psi$  by optimizing the weighted sum of the two learning objectives (Weston et al., 2012). When using gradient descent, we can optimize the combined objective in two ways: either by following the gradient with respect to the joint objective or by alternating between the gradients of the different objectives. Simultaneous learning allows to use weak contextual objectives for regularization which might not be sufficient objectives for estimating useful functions by themselves. However, this procedure introduces the need to find a good weighting of the different learning objectives, which might be difficult if the gradients of the objectives differ by orders of magnitude and vary during learning.

## 4 PATTERNS FOR CONTEXTUAL LEARNING

We will now present different contextual learning approaches, which we have grouped into patterns. We describe for each pattern the general idea, the underlying prior, the contextual data, and the contextual learning objective  $\mathcal{L}_c$ . We point to successful applications of each pattern and visualize the patterns with schemas as in Fig. 2.

**How to read the schemas:** The schemas show the functions, drawn as arrows, and the variables introduced in Section 3. Predictions of variables are indicated by  $\hat{\cdot}$ . Learning objectives are depicted in green. If variables are connected by  $\sim$ , there exists a learning objective to enforce similarity between them. The  $=$ -sign (see Fig. 6) indicates that a function is replicated (e.g. by weight sharing).

### 4.1 DIRECT PATTERN

The direct pattern leverages known, intermediate results of the computation performed by  $f$ . Given these intermediate results as contextual data  $\mathbf{c}$ , we can learn a function  $\phi$  that transforms  $\mathbf{x}$  into the representation  $\mathbf{s}$  such that  $\mathbf{s} \sim \mathbf{c}$ , as shown in Fig. 2. The pattern is only applicable if  $\mathbf{c}$  makes it easier to predict  $\mathbf{y}$ , and if  $\mathbf{x}$  contains enough information to predict  $\mathbf{c}$ . The example in Section 1 is an instance of this pattern.

To formalize this pattern, we use a suitable supervised learning objective  $\mathcal{L}_c = \mathcal{L}_{\text{direct}}(\phi | \{\mathbf{x}, \mathbf{c}\})$  that enforces the representation  $\mathbf{s}$  to be equal to the context  $\mathbf{c}$  as the contextual objective.

**Applications:** Machine learning approaches in computational biology frequently use this pattern to combine understanding from biology research with learning. For example, in contact prediction,

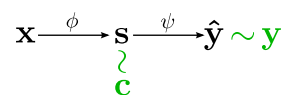


Figure 2: Direct pattern

the goal is to predict which parts of a folded protein are close to each other based on the DNA sequence that describes the protein. Virtually all learning-based approaches to this problem first predict intermediate representations  $s$ , such as secondary structures (local 3D structure categories), and then use  $s$  to predict contacts (Cheng & Baldi, 2007). The intermediate representation can be reliably estimated which greatly facilitates learning  $\phi$ .

#### 4.2 MULTI-TASK PATTERN

This pattern applies when the contextual data  $c$  are outputs of a related function (with input  $x$ ) that shares computations with the function we want to estimate. As illustrated in Fig. 3, the pattern assumes that the target function  $f = \phi \circ \psi$  and the related function  $\phi \circ \beta$  share the  $\phi$  and therefore have the same intermediate representation  $s = \phi(x)$ . By training the representation to predict both  $y$  using  $\psi$ , and  $c$  using the auxiliary learnable function  $\beta : s \rightarrow c$ , we incorporate the prior that *related tasks share intermediate representations*. This pattern corresponds to multi-task learning (Caruana, 1997).

To apply the multi-task pattern, we can use any suitable learning objective from supervised learning  $\mathcal{L}_c = \mathcal{L}_{\text{multi-task}}(\phi, \beta | \{x, c\})$  in order to learn predicting  $c$  from  $x$ .

**Applications:** Multi-task learning has been successfully applied in a wide variety of tasks (Caruana, 1997). Recently, Levine et al. (2015) showed how a robot can learn remarkable vision-based manipulation skills, such as stacking lego blocks or screwing caps onto bottles. They train a convolutional neural network to control a robot arm and regularize the computation of the intermediate representation with the auxiliary tasks of image classification and pose prediction.

A special case of the multi-task pattern exploits unrelated tasks (Romera-Paredes et al., 2012). For more details, we refer to Appendix A.2.

#### 4.3 MULTI-VIEW PATTERN

The multi-view pattern is complementary to the multi-task pattern, treating contextual data as input instead of output. It applies when  $c$  are inputs of a related function (with output  $y$ ) that share computations with  $f$ . This pattern corresponds to multi-view learning (Sun, 2013).

When we treat  $c$  as auxiliary inputs, we can use them in two different ways: explicitly by *correlating* them with the original input  $x$  (Fig. 4), or implicitly by *predicting* the target output (Fig. 5). In both cases, we learn functions  $\phi : x \mapsto s$  and  $\beta : c \mapsto s'$ , such that  $s \sim s'$ .

The **multi-view (correlation) pattern** assumes that *correlated representations computed from related inputs are a useful intermediate representation for predicting the target output*. It can be formalized with a learning objective that enforces the correlation between  $\phi(x)$  and  $\beta(c)$ , e.g. the mean squared error  $\mathcal{L}_c = \mathcal{L}_{\text{multi-view}}(\phi, \beta | \{x, c\}) = \sum_i \|\phi(x_i) - \beta(c_i)\|^2$ . If we apply the decoupled training procedure, i.e. only optimize the contextual objective, we have to add constraints, e.g. unit variance, to  $\mathcal{L}_{\text{multi-view}}$  in order to avoid the trivial solution of having a constant intermediate representation. In case  $\phi$  and  $\beta$  are linear,  $\mathcal{L}_{\text{multi-view}}$  with unit variance corresponds to Canonical Correlation Analysis (CCA).

**Applications:** The pattern is widely used in computational neuroscience to learn from multiple modalities (e.g., EEG and fMRI) or across subjects. Dähne et al. (2014) present a non-linear variant of CCA to integrate EEG signals from multiple subjects, and use it to reduce the number of labels  $y$  required to predict the mental state of a subject. Recently, Wang et al. (2015) suggested and compared various deep architectures to combine multi-task and multi-view correlation learning. They show that a deep canonically correlated auto-encoder gives superior results in a set of visual, speech, and language learning tasks.

To the best of our knowledge, all multi-view approaches in the literature employ a decoupled training procedure. We study the possibility of simultaneous learning in Section 5.1.

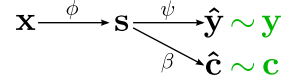


Figure 3: Multi-task pattern

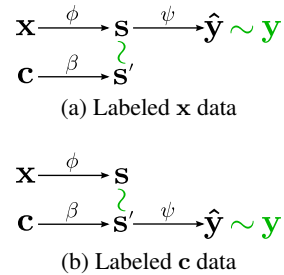


Figure 4: Multi-view (correlation) pattern

The **multi-view (prediction) pattern** is based on the prior that *predicting the target output from related inputs requires similar intermediate representations*. It trains the functions  $\phi : \mathbf{x} \mapsto \mathbf{s}$  and  $\beta : \mathbf{c} \mapsto \mathbf{s}'$  such that both  $\mathbf{s}$  and  $\mathbf{s}'$  map to the target output using the same prediction function  $\psi$ , e.g. using weight sharing. Since  $\mathbf{s}$  and  $\mathbf{s}'$  are coupled to  $\mathbf{y}$  through the main objective, we do not only regularize the representation, but also the prediction function  $\psi$ . We have not found any applications of this pattern in the literature, and provide some experimental results in Section 5.1.

#### 4.4 PAIRWISE PATTERNS

Pairwise patterns use contextual data  $\mathbf{c}_{ij}$  that carry information about the relationship between samples  $i$  and  $j$  to shape the intermediate representation (Fig. 6, the  $\parallel$  between  $\mathbf{x}_i \rightarrow \mathbf{s}_i$  and  $\mathbf{x}_j \rightarrow \mathbf{s}_j$  indicates weight sharing).

##### 4.4.1 PAIRWISE SIMILARITY/DISSIMILARITY PATTERN

If the context gives information about similarity of samples with respect to the task, we can impose the prior that *samples that are similar (dissimilar) according to their context should have similar (dissimilar) intermediate representations*. Such context is often available as information about local neighborhoods of samples (Tenenbaum et al., 2000). Another powerful source of similarity information are time sequences, since temporally subsequent samples often have similar task-relevant properties, as exploited by slow feature analysis (SFA) and temporal coherence (Wiskott & Sejnowski, 2002; Weston et al., 2012).

Similarity can be enforced with a squared loss on the distance between similar samples:

$$\mathcal{L}_{\text{similar}}(\phi | \{\mathbf{x}, \mathbf{c}\}) = \sum_{i,j} \|\phi(\mathbf{x}_i) - \phi(\mathbf{x}_j)\|^2 \mathbb{1}(\mathbf{c}_{ij} = \text{similar}), \quad (3)$$

where  $\mathbb{1}$  denotes the indicator function. Solely using this objective might lead to trivial solutions where all samples are mapped to a constant. We can resolve this problem by imposing additional balancing constraints on  $\mathbf{s}$  (Weston et al., 2012) or selectively push samples apart that are dissimilar according to the context (or optionally according to the labels  $\mathbf{y}$ ):

$$\mathcal{L}_{\text{dissimilar}}(\phi | \{\mathbf{x}, \mathbf{c}\}) = \sum_{i,j} \sigma(\|\phi(\mathbf{x}_i) - \phi(\mathbf{x}_j)\|) \mathbb{1}(\mathbf{c}_{ij} = \text{dissimilar}), \quad (4)$$

where  $\sigma$  is a function that measures the proximity of dissimilar samples in representation  $\mathbf{s}$ . Candidates for  $\sigma$  are the margin-based  $\sigma(d) = \max(0, m - d^2)$  for some pre-defined margin  $m$  (Hadsell et al., 2006), the exponential of the negative distance  $\sigma(d) = e^{-d}$  (Jonschkowski & Brock, 2014), or the Gaussian function  $\sigma(d) = e^{-d^2}$  (Jonschkowski & Brock, 2015).

**Applications:** This pattern has been shown to successfully guide the learner in identifying task-relevant properties of  $\mathbf{x}$ . Hadsell et al. (2006) show how to learn a lighting invariant pose representation of objects in the NORB dataset. Weston et al. (2012) show that regularizing a convolutional network with a temporal coherence objective outperforms pure supervised object classification in the COIL-100 dataset by 20% in terms of recognition accuracy. Jonschkowski & Brock (2015) apply the pattern in a reinforcement learning task for robot navigation, and show how leveraging temporal and robot action information enable the robot to learn a 2D state representation from raw observations, despite of the presence of visual distractors.

Note that this pattern only preserves *local* similarities between samples. If the context provides a global distance metric, Weston et al. (2012) propose to formulate contextual objectives for learning a distance-preserving mapping of  $\mathbf{x}$  to  $\mathbf{c}$  based on multi-dimensional scaling (Kruskal, 1964) or ISOMAP (Tenenbaum et al., 2000).

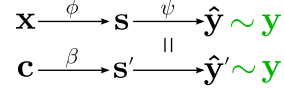


Figure 5: Multi-view (prediction) pattern

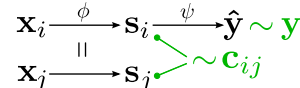


Figure 6: Pairwise pattern

#### 4.4.2 PAIRWISE TRANSFORMATION PATTERN

Instead of exploiting only binary similarity information between samples, the pairwise transformation pattern exploits continuous information about the relative transformations between samples, to make *the internal representation (or parts of it) consistent or equivariant with the known relative transformations*. Such contextual data is often available in robot and reinforcement learning setups.

Consistency with the transformations  $\mathbf{c}$  can be enforced in different ways: (a) Hinton et al. (2011) require the transformation  $\mathbf{c}$  to affect  $\mathbf{s}$  in a known way, and suggest the *transforming autoencoder model* shown in Fig. 7a to learn such an  $\mathbf{s}$ . The idea is to learn to reconstruct the transformed input from the original input and the known transformation. (b) A less strict alternative is to only assume that all transformations are linear in  $\mathbf{s}$ . Jayaraman & Grauman (2015) suggest to learn these transformations as an auxiliary task using the pattern depicted in Fig. 7b. (c) We can also turn this approach around and try to predict the transformation based on the original and the transformed representation (Agrawal et al., 2015) as depicted in Fig. 7c. All three variants (a)-(c) enforce equivariance of  $\mathbf{s}$  wrt. to the relative transformations, and can be trained using supervised contextual objective functions. (d) Instead of optimizing for equivariance, we can also enforce that the same transformation has the same effect, when applied to different samples (Fig. 7d). When transformations are discrete, we formalize this by penalizing the squared difference of the change in internal representation after applying the same transformation:

$$\mathcal{L}_{\text{transf.}}(\phi \mid \{\mathbf{x}, \mathbf{c}\}) = \sum_{i,j} \|\Delta\phi(\mathbf{x}_i) - \Delta\phi(\mathbf{x}_j)\|^2 \mathbb{1}(\mathbf{c}_i^{(\text{transf.})} = \mathbf{c}_j^{(\text{transf.})}), \quad (5)$$

where  $\Delta$  denotes the change caused by the transformation, i.e.  $\Delta\phi(\mathbf{x}_i) = \phi(\mathbf{x}_{i+1}) - \phi(\mathbf{x}_i)$  for sequential data. This objective can be extended to continuous transformations by replacing the indicator function with a similarity function  $\sigma(\mathbf{c}_i^{(\text{transf.})} - \mathbf{c}_j^{(\text{transf.})})$  from Section 4.4.1. Our earlier work uses variants of this pattern to enforce only locally consistent transformations (by multiplying  $\sigma(\phi(\mathbf{x}_i) - \phi(\mathbf{x}_j))$ ) or to enforce only consistent magnitudes of change by comparing norms  $\|\Delta\phi(\mathbf{x}_i)\|$  (Jonschkowski & Brock, 2015).

**Applications:** Many results in the literature demonstrate the usefulness of the pairwise transformation pattern. Agrawal et al. (2015) report that using relative pose information as context can reduce the error rate on MNIST by half with respect to pure supervised learning. They also demonstrate the approach for scene recognition on the SUN dataset, and show that pre-training using limited of relative pose context data is almost as good class-based supervision. Jayaraman & Grauman (2015) demonstrate a recognition accuracy of  $\approx 50\%$  on the KITTI dataset, outperforming pure supervised learning (41.81% accuracy) and SFA (47.04%).

A special case of the pairwise pattern uses contextual data to impose distance information on the label, see Appendix A.1.

## 5 EXPERIMENTS

The related work, discussed in the previous section, demonstrated that contextual learning greatly improves generalization capabilities. Our experiments complement these results by systematically comparing the different contextual patterns in two supervised learning tasks. We outline the experimental rationale and results here, and refer to Appendix B for details.

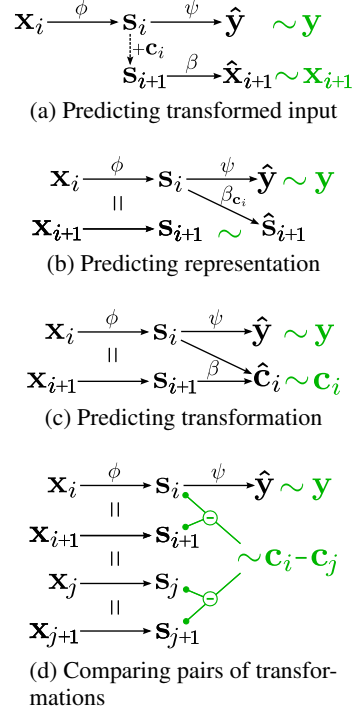


Figure 7: Pairwise transformation patterns

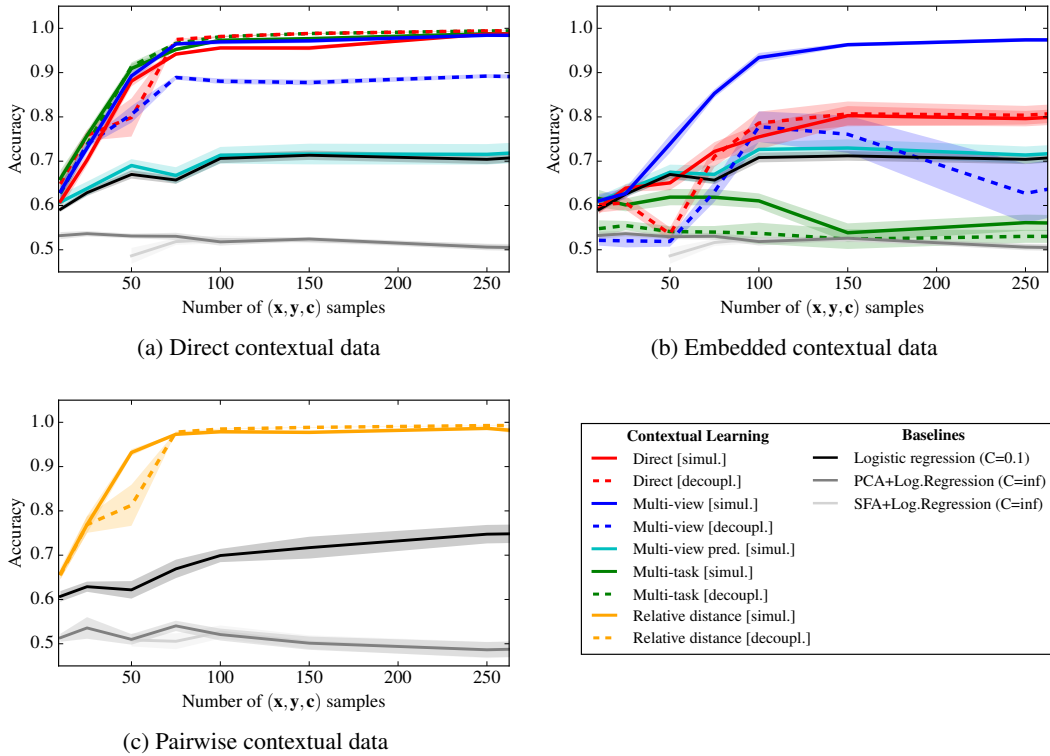


Figure 8: Experimental results for synthetic data, averaged over 10 experimental runs. The contextual variants outperform supervised and unsupervised baselines and generalize better with much less data.

### 5.1 SYNTHETIC TASK

In the first, synthetic, experiment the goal is to predict the position of a randomly moving agent in a 1-dimensional state space  $s$ . The learner cannot perceive  $s$  directly, but gets an observation  $x$ , which embeds  $s$  and a set of distractor signals in a high-dimensional space. The learned functions are linear ( $\phi$  and  $\beta$ ), and logistic functions ( $\psi$ ), respectively. We study the effect of different contextual data, patterns and training procedures on prediction accuracy. The contextual data are either (i) a noisy variant of the real state (*direct* contextual data), (ii) a second noisy high-dimensional observation (*embedded*), (iii) or a noisy variant of the agent’s actions (*pairwise*). We apply the direct, multi-view, multi-task, and pairwise transformation patterns, and perform training using the decoupled and the simultaneous procedures (pre-training is futile since we use linear functions). We compare to a supervised, and two unsupervised (PCA and SFA) baselines.

**Results:** Figure 8 shows the prediction accuracy for the different methods, based on the number of training samples. Overall, most of the contextual variants clearly outperform the baselines. We see that the best performance is achieved by applying the simultaneous training procedure, as it allows to balance task and the contextual regularization most effectively. Moreover, we see that for the embedded context, multi-task performs much worse than multi-view correlation and even than the direct pattern. The reason is that the multi-task objective of predicting the context is not suitable if the context itself contains mostly unpredictable distractors. The multi-view correlation pattern can deal with this issue, whereas the multi-view-prediction pattern works badly as it does not propagate enough information from  $\psi$  to regularize  $\phi$ .

### 5.2 HANDWRITTEN CHARACTER RECOGNITION

In this experiment, we test contextual learning for handwritten character recognition in images (see Fig. 9), where we use the pen trajectory as contextual data. In our experiments, we vary three proper-

ties: (i) the representation of the contextual data, either as continuous vectors or discrete categories, (ii) the applied pattern: direct, multi-task, or multi-view, and (iii) the training procedure: decoupled, pre-train/finetune, or simultaneous. In all our experiments, we keep the number of unlabeled data and contextual data fixed and examine how the accuracy of the main task is affected by changing the number of labeled data. All approaches use the same convolutional neural network architecture. As baselines we use purely supervised learning and unsupervised pre-training (deep auto-encoder).



Figure 9: Sample input for each of the 20 characters in this task (those written with a single stroke): a, b, c, d, e, g, h, l, m, n, o, p, q, r, s, u, v, w, y, z. Task-irrelevant variations, such as the added random lines, make this task challenging.

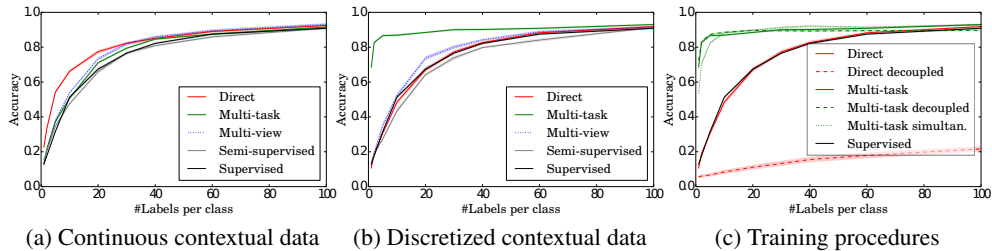


Figure 10: Contextual learning dramatically reduces the number of labels needed to solve the task. (a) uses continuous contextual data or the image in case of the semi-supervised baseline. (b) and (c) use the discretized contextual data and a similarly discretized image for the semi-supervised baseline. Lines show means, shades denote the standard errors. Line styles denote the training procedure (except for the supervised baseline, where there is only one learning objective): solid denotes pre-train/finetune, dashed lines denote decoupled training, and dotted lines denote simultaneous training.

**Results:** The results of this experiment are twofold: First, contextual learning can dramatically improve generalization in this example, achieving the same performance using 5 labels per class as the baselines achieve with 100 (see Fig. 10b). The second result is that the effectiveness of contextual learning does not only depend on the pattern and how it relates to the task and the contextual data that is available, but also on the representation of the contextual data (compare Figs. 10a and 10b).

When we use the vector of pen coordinates as context, the direct pattern provides some improvement over the baselines, but the multi-task and multi-view patterns do not improve the performance by large amounts (see Fig. 10a). However, when discretizing the trajectories into a small number of categories and applying the multi-task pattern for predicting these categories, we drastically reduce the number of labels required to solve this task (see Fig. 10b). This is not the case if we use other patterns. Moreover, we see that multi-task learning applied to the discretized context is not significantly influenced by the training procedure. The direct pattern, however, does not work if we use it with the decoupled training procedure (see Fig. 10c).

## 6 CONCLUSION AND DISCUSSION

For estimating a function from data, input/output samples are the most obvious source of information. However, for many problems there exist other data that carry important information about how the target function maps input to output. The contextual learning framework that we present allows to leverage these contextual data to improve generalization. To facilitate the application of contextual learning to novel problems, we introduce a set of contextual learning patterns, each describing a different way of exploiting contextual data. We show how related work can be cast in terms of these patterns, and also introduce novel patterns. We apply the proposed learning patterns in two supervised learning tasks and compare their effectiveness.

Our experimental evaluation demonstrates that contextual learning can substantially benefit learning, both in terms of reduced size of the training set and in terms of improved generalization. These positive effects critically depend on a suitable combination of task, contextual data, and contextual learning pattern. Investigating these interdependencies will be the focus of our future work. Moreover, we do not believe the types of contextual data and patterns presented in this paper to be exhaustive. We believe that we can find novel powerful patterns, e.g. by combining multiple patterns and including several sources of contextual data.

We believe that contextual learning can be a powerful paradigm for improving the effectiveness of learning approaches. However, most datasets available in machine learning are shaped according to the supervised learning paradigm and thus only consist of input/output samples. We therefore suggest to construct datasets that include more contextual data, and augment well-curated datasets such as ImageNet with context. Apart from that, we believe that reinforcement learning benefits most significantly from a contextual approach (Jonschkowski & Brock, 2015). Contextual learning is so effective in this setting because of the strong relationship between the different sources of data (observations, actions, and rewards over time). By formulating priors over their relationships, we can exploit these rich contextual data in order to learn better state, action and policy representations.

#### ACKNOWLEDGMENTS

We gratefully acknowledge the funding provided by the European Commission (SOMA project, H2020-ICT-645599), the German Research Foundation (Exploration Challenge, BR 2248/3-1), and the Alexander von Humboldt foundation through an Alexander von Humboldt professorship (funded by the German Federal Ministry of Education and Research). We would like to thank Marc Toussaint and the University of Stuttgart for granting us access to their GPU cluster, and Sven Dähne, Robert Lieck, and Michael Schneider for fruitful discussions and comments on this manuscript.

#### REFERENCES

Agrawal, P., Carreira, J., and Malik, J. Learning to See by Moving. *arXiv:1505.01596 [cs]*, May 2015.

Bastien, Frédéric, Lamblin, Pascal, Pascanu, Razvan, Bergstra, James, Goodfellow, Ian, Bergeron, Arnaud, Bouchard, Nicolas, Warde-Farley, David, and Bengio, Yoshua. Theano: new features and speed improvements. In *NIPS 2012 deep learning workshop*, 2012.

Caruana, R. Multitask learning. *Machine learning*, 28(1):41–75, 1997.

Cheng, J. and Baldi, P. Improved residue contact prediction using support vector machines and a large feature set. *BMC Bioinformatics*, 8(1):113, April 2007. ISSN 1471-2105.

Dähne, S., Nikulin, V. V., Ramírez, D., Schreier, P. J., Müller, K.-R., and Haufe, S. Finding brain oscillations with power dependencies in neuroimaging data. *NeuroImage*, 96:334–348, August 2014. ISSN 1053-8119.

Erhan, D., Bengio, Y., Courville, A., Manzagol, P.-A., Vincent, P., and Bengio, S. Why Does Unsupervised Pre-training Help Deep Learning? *J. Mach. Learn. Res.*, 11:625–660, 2010. ISSN 1532-4435.

Hadsell, R., Chopra, S., and LeCun, Y. Dimensionality Reduction by Learning an Invariant Mapping. In *Proc. Computer Vision and Pattern Recognition Conference (CVPR)*. IEEE Press, 2006.

Hinton, G. E., Krizhevsky, A., and Wang, S. D. Transforming auto-encoders. In *Artificial Neural Networks and Machine Learning-ICANN 2011*, pp. 44–51. Springer, 2011.

Jayaraman, D. and Grauman, K. Learning image representations equivariant to ego-motion. *arXiv:1505.02206 [cs, stat]*, May 2015.

Jonschkowski, R. and Brock, O. State Representation Learning in Robotics: Using Prior Knowledge about Physical Interaction. In *Robotics Science and Systems (RSS) X*, Berkeley, USA, 2014.

Jonschkowski, R. and Brock, O. Learning state representations with robotic priors. *Autonomous Robots*, 39(3):407–428, July 2015. ISSN 0929-5593, 1573-7527.

Kruskal, J. B. Multidimensional scaling by optimizing goodness of fit to a nonmetric hypothesis. *Psychometrika*, 29(1):1–27, March 1964. ISSN 0033-3123, 1860-0980.

Levine, S., Finn, C., Darrell, T., and Abbeel, P. End-to-End Training of Deep Visuomotor Policies. *arXiv:1504.00702 [cs]*, April 2015.

Mitchell, Tom M. *The need for biases in learning generalizations*. Department of Computer Science, Laboratory for Computer Science Research, Rutgers Univ., 1980.

Romera-Paredes, B., Argyriou, A., Berthouze, N., and Pontil, M. Exploiting unrelated tasks in multi-task learning. In *International Conference on Artificial Intelligence and Statistics*, pp. 951–959, 2012.

Silla Jr, C. N. and Freitas, A. A. A survey of hierarchical classification across different application domains. *Data Mining and Knowledge Discovery*, 22(1-2):31–72, 2010. ISSN 1384-5810.

Sun, S. A survey of multi-view machine learning. *Neural Computing and Applications*, 23(7-8):2031–2038, February 2013. ISSN 0941-0643, 1433-3058.

Tenenbaum, J. B., Silva, V. de, and Langford, J. C. A Global Geometric Framework for Nonlinear Dimensionality Reduction. *Science*, 290(5500):2319–2323, December 2000. ISSN 0036-8075.

Wang, W., Arora, R., Livescu, K., and Bilmes, J. On Deep Multi-View Representation Learning. 2015.

Weston, J., Ratle, F., Mobahi, H., and Collobert, R. Deep Learning via Semi-supervised Embedding. In Montavon, G., Orr, G. B., and Müller, K.-R. (eds.), *Neural Networks: Tricks of the Trade*, number 7700 in Lecture Notes in Computer Science, pp. 639–655. Springer Berlin Heidelberg, 2012. ISBN 978-3-642-35288-1 978-3-642-35289-8.

Williams, B. H., Toussaint, M., and Storkey, A. J. A Primitive Based Generative Model to Infer Timing Information in Unpartitioned Handwriting Data. In *IJCAI*, pp. 1119–1124, 2007.

Wiskott, L. and Sejnowski, T. J. Slow Feature Analysis: Unsupervised Learning of Invariances. *Neural Computation*, 14(4):715–770, April 2002. ISSN 0899-7667.

## A PATTERNS

In this section, we list patterns that are special cases of the patterns presented in Section 4.

## A.1 LABEL DISTANCE PATTERN

The label distance pattern is a special case of the pairwise pattern, where the context defines distances between labels, not samples (see Fig. 11). An instance of this pattern, often used in structured prediction, is hierarchical multi-class learning (Silla Jr & Freitas, 2010), where a hierarchy is imposed on the labels to penalize misclassifications between samples with similar classes less severely.

## A.2 IRRELEVANCE PATTERN

All patterns discussed so far only use contextual data that are related to the main learning task in a positive sense. Romera-Paredes et al. (2012) show how to exploit knowledge about unrelated tasks, by enforcing the context to be orthogonal to the representation for the main task. The authors formalize this idea in a multi-task learning scenario by forcing  $\psi$  to be orthogonal to the auxiliary-task predictions  $\beta_i$  (see Fig. 12) which allows to use knowledge about irrelevant distractors present in the input data. However, it is unclear how to efficiently formulate the orthogonality constraints between  $\psi$  and  $\beta_i$  for the non-linear case, in order to exploit this pattern in deep learning.

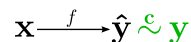


Figure 11: Label distances

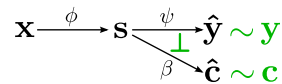


Figure 12: Exploiting irrelevant context.

## B EXPERIMENTAL METHODS

The implementation of our experiments is based on Theano (Bastien et al., 2012) and Lasagne<sup>1</sup>.

### B.1 SYNTHETIC TASK

**Task:** The task consists of an agent moving randomly through a 1-dimensional state space  $s_t \in \mathbb{R}$  where  $t$  denotes the time index. The space is split into two regions  $O_1 = \{s \mid s > 0\}$  and  $O_2 = \{s \mid s < 0\}$  and the goal of the learner is to determine in which of the two regions the agent is located. However, the learner cannot observe the state space directly, it only gets  $d$ -dimensional observations which are obfuscated by  $d - 1$  distractors  $u_t^{(i)}$ ,  $i \in \{1, \dots, d - 1\}$ : the observation is generated by applying a random rotation  $\mathbf{R}$  to the concatenated state and distractor vector:  $\mathbf{x}_t = \mathbf{R} [s_t, u_t^{(1)}, \dots, u_t^{(d-1)}]$ . In every time step, both the state as well as the distractor dimensions change randomly:  $s_{t+1} = s_t + \varepsilon_t^{(s)}$ ,  $u_{t+1}^{(i)} = u_t^{(i)} + \varepsilon_t^{(i)}$ , where  $\varepsilon_t^{(s)}, \varepsilon_t^{(i)} \sim \mathcal{N}(0, 1)$ . In addition the agent receives a supervised signal  $\mathbf{y}$  which is 0 if the agent is in region  $O_1$  and 1 in zero  $O_2$ .

**Baselines:** We compare the contextual learning variants to a supervised method (logistic regression mapping  $\mathbf{x}$  directly to  $\mathbf{y}$ ) and to two unsupervised methods. For the unsupervised baselines we apply either PCA or SFA to learn a 1-dimensional  $\mathbf{s}$ , and then train a logistic regression mapping from  $\mathbf{s}$  to  $\mathbf{y}$ . For the logistic regression, we use  $L_2$  regularization with  $C \in \{0.001, 0.01, 0.1, 1.0, \infty\}$  and choosing the result with the lowest test error. (Note that we do not apply  $L_2$  regularization for training the contextual variants.)

**Contextual Patterns:** We implemented the four principal contextual patterns from Section 4, using a linear function for  $\phi(\mathbf{x}) = \mathbf{w}_\phi^T \mathbf{x} = \mathbf{s}$  and a logistic function for  $\psi(\mathbf{s}) = \frac{1}{1+e^{-\mathbf{w}_\psi^T \mathbf{s}}}$ . We apply Stochastic Gradient Descent with Nesterov momentum with value 0.9 to learn  $\phi$  and  $\psi$  using a logistic regression loss in addition to the contextual objective. We train each pattern using the decoupled and simultaneous training procedures (pre-train/fine-tune is futile due to the linearity of  $\phi$  and  $\psi$ , see Section 3.1).

For the **direct pattern**, we learn  $\phi$  directly by performing a linear regression on  $\mathbf{c}$ , using the mean squared error loss. When training simultaneously, we weigh the main and the contextual objective equally.

We implement the **multi-task pattern** by using a linear function  $\beta(\mathbf{s}) = \mathbf{w}_\beta^T \mathbf{s}$  for the auxiliary task and optimize it using linear regression. Again, we weigh the main and the contextual objective equally.

We implement two versions of the **multi-view pattern**: first, the **correlation** variant, using  $\beta(\mathbf{c}) = \mathbf{w}_\beta^T \mathbf{c} = \mathbf{s}'$ , optimizing for  $\mathbf{s} \approx \mathbf{s}'$ , secondly, the **prediction** variant. For the correlation pattern we have to give weight 0.99 to the supervised and 0.01 to the contextual objective, since the gradients from the contextual MSE loss and the supervised softmax loss differ by several orders of magnitude.

Finally, we implement the **pairwise pattern**, in form of the transformation pattern. We use a simplified version of the variant depicted in Fig. 7c with a fixed auxiliary function  $\beta(\mathbf{s}_i, \mathbf{s}_j) = \mathbf{s}_i - \mathbf{s}_j$ . Again, we weigh the main and the contextual objective equally.

We evaluate subsets of the implemented patterns with three types of contextual data. In each experiment, we use different amounts of  $(\mathbf{x}, \mathbf{y}, \mathbf{c})$  triplets for learning, and test the prediction accuracy in the main task for a test set of size 50000. The dimensionality of  $\mathbf{x}$  is set to 50. We average the results over 10 independently generated training and test sets.

**Direct Contextual Data:** First, we provide the learner with very informative data in the form of a noisy variant of the real state:  $\mathbf{c}_t^{(s)} = s_t + \varepsilon_t^{(s)}$ , with  $\varepsilon_t^{(s)} \sim \mathcal{N}(0, 0.05)$ . Figure 8a shows that all contextual learners except for the multi-view-prediction pattern generalize well, even given low amounts of data. The unsupervised methods fail to extract a good state representation since the real hidden  $\mathbf{s}$  neither exhibits high variance, nor a slower trajectory than the distractors. Pure supervised logistic regression works better, but even when doubling the number of  $(\mathbf{x}, \mathbf{y})$  pairs, it does not reach the performance of the contextual methods. We believe that the multi-view-prediction pattern works badly because it does not propagate enough information from the learned  $\psi$  to regularize  $\phi$ .

<sup>1</sup><https://github.com/Lasagne/Lasagne>

**Embedded Contextual Data:** In the second experiment, we provide context corresponding to an additional, noisy sensor view by mapping the state into a different  $e$ -dimensional observation space,  $\mathbf{c}_t^{(v)} = \mathbf{Q} [s_t + \varepsilon_t^{(v)}, v_t^{(1)}, \dots, v_t^{(e-1)}]$  with distractors  $v_t^{(i)}$ , random rotation matrix  $\mathbf{Q}$  and  $\varepsilon_t^{(v)} \sim \mathcal{N}(0, 0.05)$ . In the experiments, we set  $e = \frac{d}{2}$ . Figure 8b shows that most contextual variants still outperform the supervised method, but need more data to generalize well due to the less informative context. The multi-view method performs best, whereas the multi-task performs even worse than logistic regression. Moreover, we see that the simultaneous training procedures outperform the decoupled variants, most drastically in the multi-view pattern.

**Relative Contextual Data:** The last type of data corresponds to a noisy variant of the “actions”,  $\mathbf{c}_t^{(a)} = s_t - s_{t-1} + \varepsilon_t^{(a)}$  with  $\varepsilon_t^{(a)} \sim \mathcal{N}(0, 0.05)$ . Fig. 8c shows clearly that this context is highly informative, and allows to learn from few samples.

## B.2 HANDWRITTEN CHARACTER RECOGNITION

**Dataset and task:** The dataset for this experiment is based on the character trajectories dataset<sup>2</sup>, which consists of time series of pen velocities in x and y direction and pen tip force (more details in Williams et al. (2007)). The dataset includes 20 characters that can be written in a single stroke. Based on this dataset, we generate monochrome images of size  $32 \times 32$  pixels. During image generation, we add different variations to make this task more challenging. We trace the character trajectories with varying pen width, we translate the characters randomly, and we overlay distracting lines that connect three random points in the image (see Fig. 9). These images form the input  $\mathbf{x}$  for this task. Additionally, we generate context data in the form of coordinates of 32 points along the character trajectory making up a 64D vector  $\mathbf{c}$ . Unlike the input images, these points are not translated. The task is to recognize which of the 20 characters is in the given image. The training data consist of 100 input/context pairs per character, a random subset of which are labeled. In our experiment, we vary the number of labels per character from 1 to 100.

**Neural network structure and training:** We use a convolutional neural network (CNN) with rectified linear units (ReLU). We first apply a convolution with 32 filters of size  $5 \times 5$  followed by ReLU non-linearity and max-pooling. The same sequence is repeated, followed by 50% dropout and a fully connected layer of 32 ReLUs (the intermediate representation  $\mathbf{s}$ ). This is again followed by a 50% dropout and 20 softmax output units. The entire network has 52756 parameters. The supervised task is formulated using the categorical crossentropy loss and optimized using Nesterov momentum with learning rate 0.003, momentum 0.9, and batch size 20 for 100 epochs, followed by 10 epochs with learning rate 0.0003. All experiments are repeated 10 times.

**Discretization:** In the experiment, we test two different representations of the contextual data. The original continuous vector representation and a discretization into 32 classes, which we obtain with k-means clustering. The rationale behind the discretization is that the exact trajectory cannot be recovered from the image (because it is not clear from the image where the character trajectory starts). We tested the same discretization on the image in the semi-supervised baseline.

**Applied patterns:** We compare the direct pattern, the multi-task pattern, and the multi-view pattern. The direct pattern uses a mean-squared-error objective to enforce the intermediate representation to be equal to a 32D version of the pen trajectory or the one-hot-vector that corresponds to the discretized trajectory. The multi-task pattern incorporates an additional network layer to predict the context, either a linear layer with mean-squared-error loss to predict the trajectory or a softmax layer with cross-entropy loss to predict its discretization. The multi-view pattern uses two ReLU-layers with 32 units and dropout to compute the intermediate representation  $\mathbf{s}'$  which we tie to  $\mathbf{s}$  with a mean-squared-error objective. Since this objective creates trivial solutions if trained independently, we optimize it simultaneously with the main objective (weighing them with 0.05 and 0.95, respectively). All other patterns are trained using the pretrain/finetune procedure unless indicated otherwise. For simultaneous training of the multi-task pattern, we used uniform weighting.

**Baselines:** We compare against supervised learning on the labeled data and semi-supervised baselines: In the continuous case, we reconstruct the image using a convolutional autoencoder that mirrors the structure of the convolutional network. In the discrete case we use a similar structure as for multi-task learning but predict the discretized image instead of the discretized trajectory.

<sup>2</sup><https://archive.ics.uci.edu/ml/datasets/Character+Trajectories>